S.Fig.1 **ACUTE CHARACTERISTICS**

	All n=71	Mild n=29	Moderate N=22	Severe n=20	p value (<0.05)
Age	61.1 (2.0)	59.2 (3.7)	59.6 (3.3)	66.3 (3.1)	NS
Sex (M:F)	1.1	1.01	0.82	1.71	NS
Ethnicity (Caucasian %)	87.3 %	92.6 %	68.2 %	100 %	p<0.05
BMI	29.3 (1.1)	26.3 (2.1)	31.3 (2.2)	31.2 (1.8)	NS
Hypertension	41.4 %	63.2 %	50 %	40 %	NS
IHD	5.6 %	3.4 %	13.6 %	5.0 %	NS
Pulmonary[†]	16.9 %	24.1 %	9.1 %	15.0 %	NS
Asthma	22.5 %	17.2 %	27.3 %	26.3 %	NS
Diabetes	29.6 %	17.2 %	22.7 %	55.0 %	p<0.05
Bacterial infection	23.9 %	13.8 %	27.3 %	35.0 %	NS
PE	5.6 %	3.4 %	4.5 %	10.0 %	NS
AKI	8.5 %	10.3 %	0.0 %	15.0 %	NS
CRP	121.8 (12.1)	60.6 (15.3)	136.4 (21.7)	220.5 (27.2)	p<0.001
LOS (days)	23.7 (3.8)	24.4 (6.3)	13.1 (3.2)	35.9 (11.1)	p<0.001
30 day mortality (alive/deceased)	12.7 %	0.0 %	0.0 %	45.0 %	p<0.001

Supplementary Figure 1.

Acute (inpatient) cohort characteristics. Abbreviations as follow: IHD, ischaemic heart disease; BMI, body mass index; AKI, acute kidney injury; PE, pulmonary emboli; CRP, C-reactive protein; LOS, length of stay. † Pulmonary disease includes chronic pulmonary diseases excluding asthma. Values in ( ) represent standard error of the mean.

A

Marker	Category	Function
CXCR1	Chemokine receptor	Binds CXCL8/IL-8; migration to peripheral tissues via chemotaxis
CXCR2	Chemokine receptor	Binds CXCL8/IL-8; migration to peripheral tissues via chemotaxis
CXCR4	Chemokine receptor	Monocyte retention in bone marrow and infiltration of peripheral tissues
CXCR6	Chemokine receptor	Migration towards ligand CXCL16 which is expressed at high levels in the lung
CCR7	Chemokine receptor	Migration towards secondary lymphoid tissue
CCR8	Chemokine receptor	Migration towards secondary lymphoid tissue
PSGL1	Adhesion molecule	Facilitates leucocyte rolling on vascular endothelium to exit bloodstream
CD62L/L-Selectin	Adhesion molecule	Facilitates leucocyte tethering and rolling on vascular endothelium to exit bloodstream
CD31/PECAM-1	Adhesion molecule	Facilitates leucocyte migration through vascular endothelial junctions/endothelial transmigration into peripheral tissues
Integrin β7	Integrin	Dimerises with integrin α4 for leucocyte migration to mucosal tissues, towards MAdCAM-1 on mucosal epithelia, and interacts with extra-cellular matrix (ECM) components
VLA-4/Integrin α4β1	Integrin	Facilitates leucocyte interactions with vascular endothelia and ECM components for migration through endothelial and connective tissue barriers
TNFα	Inflammatory mediator	Induced by pattern recognition receptor (PRR) mediated activation of monocytes, inflammatory immune responses and tissue repair
IL-1β	Inflammatory mediator	Induced by pattern recognition receptor (PRR) mediated activation of monocytes, inflammatory immune responses and tissue repair
COX-2	Inflammatory mediator	Induced by pattern recognition receptor (PRR) mediated activation of monocytes, contributes to inflammation by generating prostaglandins from conversion of arachidonic acid.

B

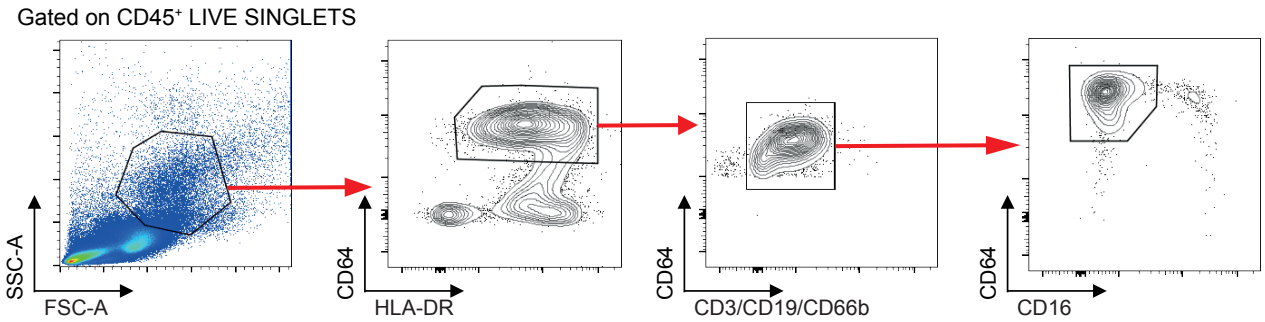

C

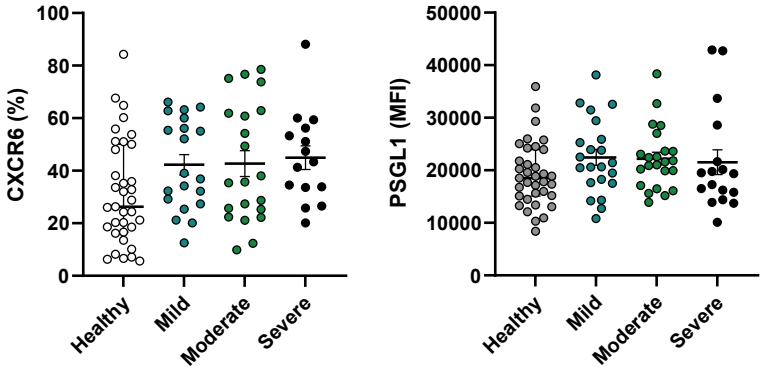

D

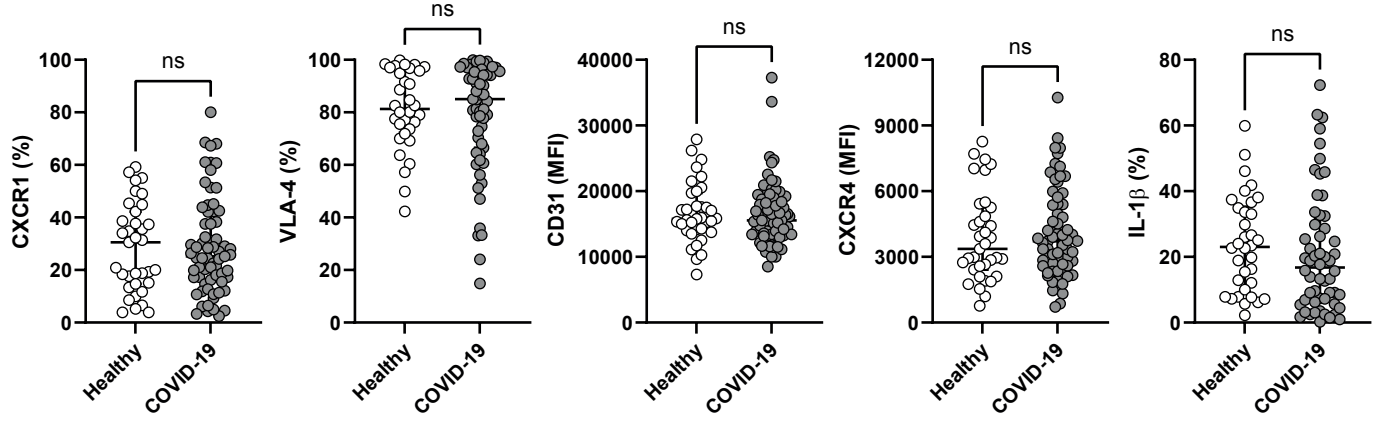

Supplementary Figure 2.

(A) Table describing functions of leucocyte migration markers and inflammatory mediators produced in response to microbial stimulation, as assessed on monocytes in COVID-19 patients. **(B)** Representative FACS plots outlining flow cytometric gating strategy used for analysis of monocytes within PBMC samples: pre-gated on live $CD45^+$ cells, circulating classical $CD14^+$ monocytes were identified as $HLA\text{-}DR^+CD64^+$ $CD3^-CD19^-CD66b^-$ $CD16^-$ cells expressing CD14. **(C)** Graphs show frequencies of $CD14^+$ monocytes expressing CXCR6 and $CD14^+$ monocyte expression level of PSGL-1 as determined by mean fluorescence intensity (MFI) from healthy individuals (n=35) and acute COVID-19 patients with mild (CXCR6: n=20; PSGL-1: n=22), moderate (CXCR6: n=21; PSGL-1: n=23) and severe (CXCR6: n=15; PSGL-1: n=17) disease. Graphs show individual patient data with bar representing median $\pm$ interquartile range. Kruskal Wallis with Dunn's post hoc test. **(D)** Graphs show frequencies of $CD14^+$ monocytes expressing CXCR1, VLA-4 and producing IL-1β and $CD14^+$ monocyte levels of expression of CD31 and CXCR4 as determined by mean fluorescence intensity in healthy individuals (CXCR1: n=35; VLA-4: n=32; CD31: n=35; CXCR4: n=35; IL-1β: n=34) and total acute COVID-19 patients (CXCR1: n=67; VLA-4: n=59; CD31: n=67; CXCR4: n=66; IL-1β: n=56). Graphs show individual patient data with bar representing mean $\pm$ standard error of the mean (CD31, CXCR4) or median $\pm$ interquartile range (CXCR1, VLA-4, IL-1β). Unpaired *t*-test (CD31, CXCR4), Mann-Whitney test (CXCR1, VLA-4, IL-1β).

S.Fig.3

CONVALESCENT CHARACTERISTICS

	All (n=142)	No breathlessness (n=70)	Shortness of breath (n=68)	No fatigue (n=73)	Fatigue (n=63)	p value (<0.05)	
						SOB	Fatigue
Mild (n=)	28	18	10	14	12		
Moderate (n=)	50	20	27	26	22		
Severe (n=)	64	32	29	33	28	NS	NS
Age	58.3 (1.1)	57.4 (1.6)	59.1 (1.5)	58.5 (1.6)	58.1 (1.5)	NS	NS
Sex (M:F)	1.73	1.69	1.77	1.68	1.72	NS	NS
Ethnicity (Caucasian %)	76.8 %	67.1 %	86.1 %	76.0 %	77.9 %	<0.01	NS
BMI	31.1 (0.5)	30.4 (0.8)	31.8 (0.6)	31.5 (0.7)	30.8 (0.7)	NS	NS
Hypertension	34.5 %	34.3 %	34.7 %	33.8 %	34.7 %	NS	NS
IHD	9.2 %	8.6 %	9.7 %	12.1 %	5.9 %	NS	NS
Pulmonary[†]	12.0 %	12.9 %	11.1 %	16.0 %	7.4 %	NS	NS
Asthma	21.8 %	17.1 %	26.4 %	18.7 %	26.5 %	NS	NS
Diabetes	12.7 %	14.3 %	11.1 %	13.3 %	11.8 %	NS	NS
Bacterial infection	14.8 %	12.9 %	16.7 %	17.3 %	13.2 %	NS	NS
PE	4.2 %	7.1 %	1.4 %	4.0 %	4.4 %	NS	NS
AKI	7.8 %	2.86 %	12.5 %	8.5 %	7.4 %	NS	NS
CRP	161.6 (9.6)	160 (13.8)	164 (15.3)	159 (15.6)	164 (13.6)	NS	NS
Length of stay	15.7 (1.8)	16.3 (3.0)	15.0 (1.9)	12.4 (1.7)	18.6 (3.0)	NS	NS
Time to follow up (days)	151.4 (3.4)	150 (4.7)	152 (5.0)	159 (5.2)	145 (4.5)	NS	<0.05
Radiology (abnormal %)	31.0 %	22.9 %	44.4 %	30.7 %	38.2 %	<0.01	NS

Supplementary Figure 3.

Convalescent COVID-19 follow up cohort lung function tests at the time of their outpatient visit. 102 of 142 patients had lung function performed. Results are presented according to the presence, or absence, of new fatigue, shortness of breath or radiological abnormality at the time of follow up. Units of measurement: FEV_1, litres/min; FVC, litres; millilitres CO/minute/mm Hg. Values in ( ) represent standard error of the mean. % predicted is a comparison to the GLI (2017) reference values.

S.Fig.4

CONVALESCENCE PROFILES

	FEV_1	FEV_1 % predicted	FVC	FVC % predicted	FEV_1/FVC %	DLCO	DLCO % predicted
All (n=102)	2.73 (0.08)	87.9 (2.14)	3.51 (0.10)	90.9 (1.71)	78.2 (0.90)	6.84 (0.35)	87.9 (1.66)
Lung function- breathlessness outcome							
No breathlessness (n=44)	2.83 (0.13)	93.2 (2.97)	3.58 (0.16)	93.7 (2.89)	79.1 (1.35)	6.64 (0.44)	86.6 (2.76)
Shortness of breath (n=58)	2.65 (0.09)	84.0 (2.97)	3.45 (0.12)	88.8 (2.08)	77.4 (1.24)	6.97 (0.54)	88.8 (2.23)
Breathlessness p value (<0.05)	NS	<0.05	NS	NS	NS	NS	NS
Lung function- fatigue outcome							
No fatigue (n=46)	2.67 (0.12)	86.5 (2.55)	3.39 (0.16)	87.3 (2.66)	79.2 (1.39)	6.08 (0.45)	94.1 (2.89)
Fatigue (n=56)	2.78 (0.09)	89.1 (3.34)	3.60 (0.12)	93.8 (2.21)	77.3 (1.21)	7.40 (0.53)	89.3 (2.01)
Fatigue p value (<0.05)	NS	NS	NS	0.06	NS	0.07	NS
Lung function-radiological outcome							
Radiology resolved (n=63)	2.75 (0.10)	87.7 (3.01)	3.56 (0.13)	92.4 (2.16)	77.3 (1.2)	7.44 (0.51)	90.0 (2.13)
Radiology abnormal (n=39)	2.69 (0.11)	88.3 (2.70)	3.40 (0.14)	88.3 (2.74)	79.6 (1.3)	5.88 (0.35)	84.6 (2.56)
Abnormal radiology p value (<0.05)	NS	NS	NS	NS	NS	<0.05	0.06

Supplementary Figure 4.

Convalescent COVID-19 follow up cohort lung function tests at the time of their outpatient visit. 102 of 142 patients had lung function performed. Results are presented according to the presence, or absence, of new fatigue, shortness of breath or radiological abnormality at the time of follow up. Units of measurement: FEV1, litres/min; FVC, litres; millilitres CO/minute/mm Hg. Values in ( ) represent standard error of the mean. % predicted is a comparison to the GLI (2017) reference values.

A

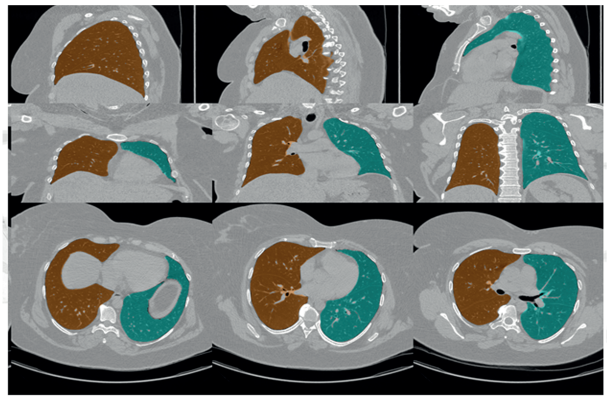

Automated CT scan lung segmentation

Lung texture analysis (LTA)

B

Asymptomatic

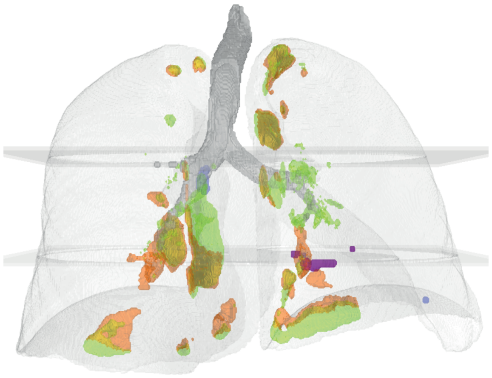

Symptomatic

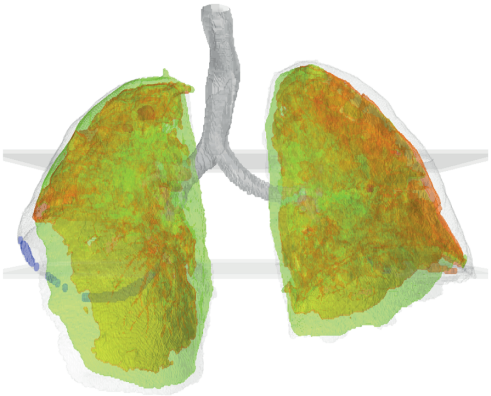

Hyperlucency Ground glass Reticulations Honeycombing

C

Lung density analysis (LDA)

Asymptomatic

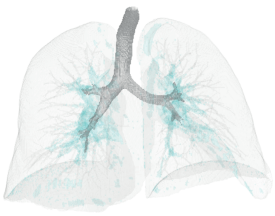

Very high density High density

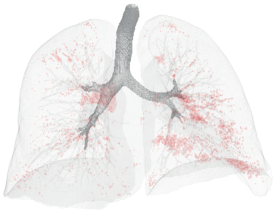

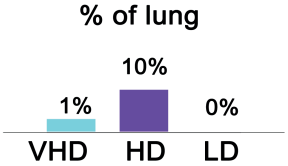

Low density

Symptomatic

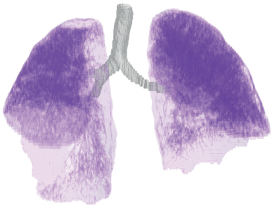

Very high density High density

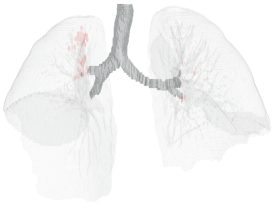

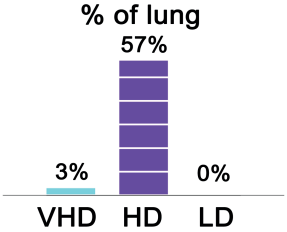

Low density

Supplementary Figure 5.

Quantitative CT analysis in symptomatic convalescent COVID-19 patients. CT scan images from 12 convalescent patients with breathlessness and/or fatigue, taken at outpatient follow up appointments, were analysed using lung texture analysis and lung densitometry analysis+ software algorithms (Imbio, USA). **(A)** Automated lung segmentation in sagittal (top row), coronal (middle row) and transverse (bottom row) planes. **(B)** Example of lung texture analysis in asymptomatic (no breathlessness or fatigue) and symptomatic (breathless and/or fatigued) patients enabling identification of types of lung damage including hyperlucency, ground glass changes, reticulations and honeycombing. **(C)** Example of lung density analysis in asymptomatic and symptomatic patients, enabling identification of high density and very high density representing ground glass changes and inflammation, respectively. On average, 57% of lungs of symptomatic patients displayed high density changes (ground glass changes) compared to 10% of asymptomatic patients.

A

Symptomatic post COVID-19 quantitative CT thorax (n=12)		
Demographics	Age (years)	58.9 (6.9)
	Sex (Male %)	62.5
	Ethnicity (% white)	75
	BMI	30.7 (3.69)
Acute data	Inpatient severity (% total) FiO_2 0.21-0.28 FiO_2 0.28-0.6 FiO_2 >0.6	Mild 12.5 Moderate 37.5 Severe 50
	CRP	166.5 (125.4)
	Length of stay (days)	18.8 (14.1)
Comorbidities	Hypertension (%)	62.5
	IHD (%)	25.0
	Chronic pulmonary disease† (%)	25
	Asthma (%)	25
	Diabetes (%)	12.5
Follow up data	Abnormal radiology at follow up (%)	62.5
	Breathless at follow up	50
	Fatigue at follow up	62.5
	Time to follow up (days)	143 (40.9)

B

Symptomatic post COVID-19 quantitative CT thorax (n=12)		
Quantitative CT Analysis	Hyperlucency, total %	0 (0, 1)
	Hyperlucency, maximum focal %	2 (0, 3.25)
	Ground glass, total %	30.5 (2, 65.8)
	Ground glass, maximum focal %	56 (4.25, 91)
	Reticulation, total %	7.5 (2.25, 13.75)
	Reticulation, maximum focal %	13 (2, 19.5)
	Honeycombing, total %	0 (0, 0)
	Honeycombing, maximum focal %	0 (0, 0)
	Low density total %	1 (0-4)
	Low density maximum focal %	0 (0-5)
	High density total %	30 (13-49)
	High density maximum focal %	39 (13-65)
	Very high density total %	2 (1-3)
	Very high density maximum total %	3 (3-5)
	CT follow-up time, days	157.8 (28.7)

Supplementary Figure 6.

(A) Convalescent COVID-19 follow up patient information for quantitative CT analysis. Abbreviations as follow: IHD, ischaemic heart disease; BMI, body mass index; CRP, C-reactive protein; † Pulmonary disease includes chronic pulmonary diseases excluding asthma. Values in ( ) represent standard error of the mean. **(B)** Different types of lung damage in 12 symptomatic convalescent COVID-19 patients as generated by automated quantitative CT analysis.

A

	Controls (n=17)	Viral (n=10)	PFILD (n=14)
Mild (n=) **Moderate (n=)** **Severe (n=)**		5 4 1	
Age	52.9 (4.4)	56 (5.7)	73.5 (1.5)
Sex (M:F)	0.47	1.0	3.67
Ethnicity (Caucasian %)	100.0	60.0	92.9
BMI	25.0 (0.86)	29.8 (3.4)	31.3 (2.1)
Hypertension	11.8 %	20.0 %	53.8 %
IHD	0.0 %	10.0 %	14.3 %
Pulmonary†	35.3 %	30.0 %	42.9 %
Asthma	0.0 %	40.0 %	21.4 %
Diabetes	0.0 %	20.0 %	14.3 %
CRP		47.2 (13.6)	
Length of stay (days)		6.7 (2.3)	
Time to follow up (days)		155.1 (7.8)	
Breathless (%)	0.0	50.0	100.0
Fatigue (%)	0.0	40.0	21.4

B

	FEV_1	FEV_1 % predicted	FVC	FVC % predicted	FEV_1/FVC %	DLCO	DLCO % predicted
PFILD (n=13)	2.23 (0.18)	83.3 (4.2)	2.68 (0.21)	77.8 (3.69)	87.5 (4.48)	3.51 (0.30)	50.4 (4.28)

Supplementary Figure 7.

(A) Control, viral (n=4 Influenza A, n=6 Respiratory Syncytial Virus) and progressive fibrosing interstitital lung disease (PFILD) characteristics. Abbreviations as follow: IHD, ischaemic heart disease; BMI, body mass index; CRP, C-reactive protein; LOS, length of stay. † Pulmonary disease includes chronic pulmonary diseases excluding asthma. Values in ( ) represent standard error of the mean. **(B)** PFILD lung function tests at the time of diagnosis of progressive phenotype. Units of measurement: FEV_1, litres/min; FVC, litres; millilitres CO/minute/mm Hg. Values in ( ) represent standard error of the mean. % predicted is a comparison to the GLI (2017) reference values.

S.Fig.8

STUDY OUTLINE

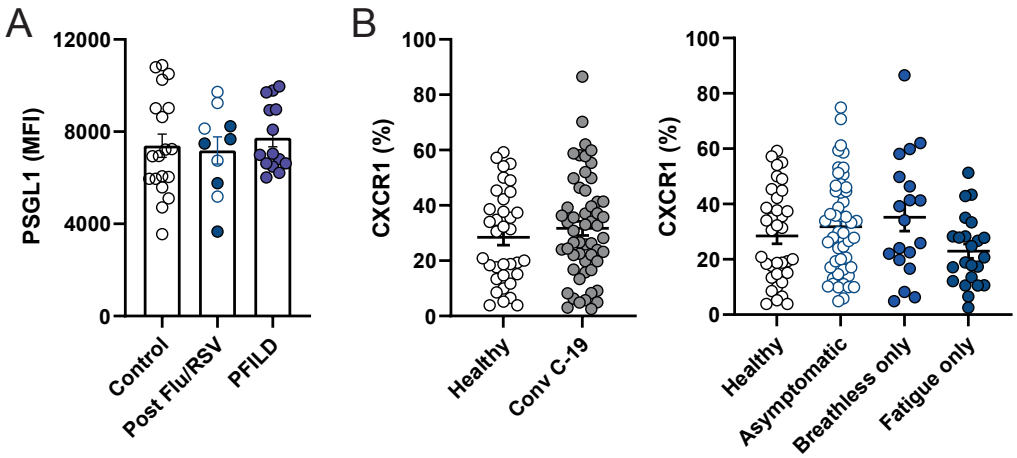

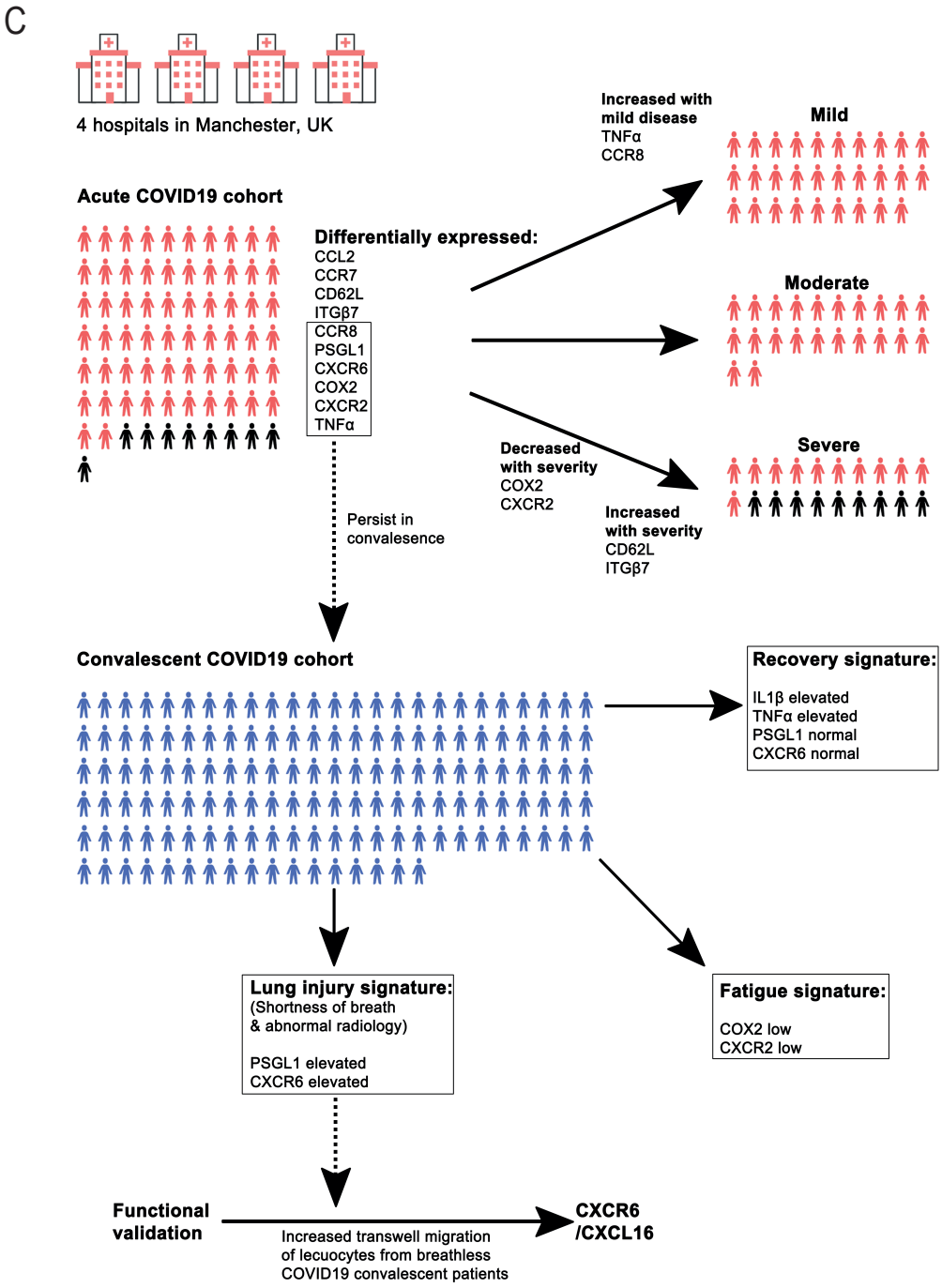

Supplementary Figure 8.

(A) Graph showing $CD14^+$ monocyte expression level of PSGL-1 as determined by mean fluorescence intensity (MFI) from healthy individuals (n=19), total convalescent flu/RSV patients (n=10) and total PFILD patients (n=14). Patients with convalescent flu/RSV were stratified into breathless (n=5, filled circles) and not breathless (n=5, open circles) within the same group. Graphs show individual patient data with bar representing median ± interquartile range. Kruskal Wallis with Dunn's post hoc test. **(B)** Graphs show frequencies of $CD14^+$ monocytes expressing CXCR1 from healthy individuals (n=35) and total convalescent COVID-19 patients (n=133). Patients with convalescent COVID-19 were also stratified into asymptomatic (no breathlessness or fatigue: n=51), breathless only (breathless but not fatigued: n=19), fatigue only (fatigued but not breathless: n=23). Graphs show individual patient data with bar representing mean ± S.E.M. Unpaired *t*-test (healthy versus convalescent COVID-19), One-way ANOVA with Holm-Sidak post hoc test (long COVID symptoms). **(C)** Summary schematic demonstrating severity-specific abnormal monocyte features in acute COVID-19 and distinct monocyte signatures corresponding to specific long COVID phenotypes.